2023

# Iterative near-term forecasting of the terrestrial carbon cycle at Harvard Forest

BOSTON UNIVERSITY

GRADUATE SCHOOL OF ARTS AND SCIENCES

Thesis

# ITERATIVE NEAR-TERM FORECASTING OF THE TERRESTRIAL CARBON CYCLE AT HARVARD FOREST

by

**ALEXIS ROSE HELGESON**

B.A., Mount Holyoke, 2020

Submitted in partial fulfillment of the

requirements for the degree of

Master of Arts

2023

Approved by

First Reader

Michael Dietze, Ph.D.
Professor of Earth and Environment

Second Reader

Lucy Hutyra, Ph.D.
Professor of Earth and Environment

Third Reader

Sparkle L. Malone, Ph.D.
Assistant Professor of Ecosystem Carbon Capture
Yale University

## DEDICATION

I would like to dedicate this work to my friends and family for their constant love and support, especially to my mother for always taking my phone calls.

## ACKNOWLEDGMENTS

This work would not have been possible without the support of current and former members of the Dietze Lab as well as members of the Harvard Forest community. Thank you to Bill Munger for allowing me access to the EMS flux tower measurements for 2021. All the code used in this research is the result of years of hard work from the PEcAn community. This research was funded as part of the NASA Carbon Monitoring Systems (CMS) project entitled “Multisensor data assimilation to support terrestrial carbon cycle and disturbance Monitoring, Reporting, Verification, and Forecasting”. Special thank you to former Harvard Forest REUs Cristina Francis and Xuan Wilson who worked on the initial condition code in 2021.

**ITERATIVE NEAR-TERM FORECASTING OF THE TERRESTRIAL CARBON CYCLE AT HARVARD FOREST**

**ALEXIS ROSE HELGESON**

ABSTRACT

Through a combination of fossil fuel emissions, land use change, and other anthropogenic activities, mankind has dramatically altered global biogeochemical cycles, leading to an unprecedented era of rapid environmental change. To anticipate how the carbon and water cycles will change in the future, and inform decisions about how to adapt and mitigate these changes, we need a better understanding of the inherent predictability of these cycles. To begin to address this challenge I designed, implemented, and analyzed a 35-day iterative forecasting workflow using Harvard Forest as an initial testbed. A key aim of this forecast is to understand the predictability of leaf area index (LAI), net ecosystem exchange (NEE), and latent heat flux (LE), which I assess in terms of how forecast uncertainty changes as a function of forecast lead time, and how the predictability of LAI, NEE and LE is impacted by the assimilation of MODIS LAI observations. I used four metrics of uncertainty (root mean square error, bias, continuous ranked probability score, and mean absolute error) to evaluate the forecast performance. Uncertainty in LAI, LE, and NEE was not positively correlated with forecast lead time. The inclusion of MODIS LAI observations improved predictability of NEE and LE, but had the greatest impact on LAI (~50% uncertainty reduction). Carbon stores (LAI as a proxy for leaf carbon) were more predictable than terrestrial fluxes (NEE, LE).

## TABLE OF CONTENTS

## LIST OF FIGURES

## Introduction

Our current understanding of the natural terrestrial carbon cycle broadly includes a large net carbon sink between the land and atmosphere and a smaller net carbon source due to land use and disturbance. Water acts as a driver for carbon cycling within ecosystems through photosynthesis, where water is lost from ecosystems as evapotranspiration (ET) and carbon is assimilated into leaves (Baldocchi et al., 2018; Beer et al., 2010). There is a large body of research estimating global carbon budgets, along with sources of spatial or temporal variability in the carbon and water cycles (Beer et al., 2010; Friedlingstein et al., 2022; Houghton, 2003). But if we want to know what the future of the terrestrial carbon cycle will be then we must evaluate our ability to predict these dynamics. While there are many studies modeling the terrestrial carbon and water cycles using hindcasts/re-analysis or long-term projections under different climate scenarios, I seek to use true forecasts, over near-term timescales that can be empirically validated, to understand the inherent predictability of these processes (Dokoohaki et al., 2021; Tian et al., 2022; Zeng et al., 2008).

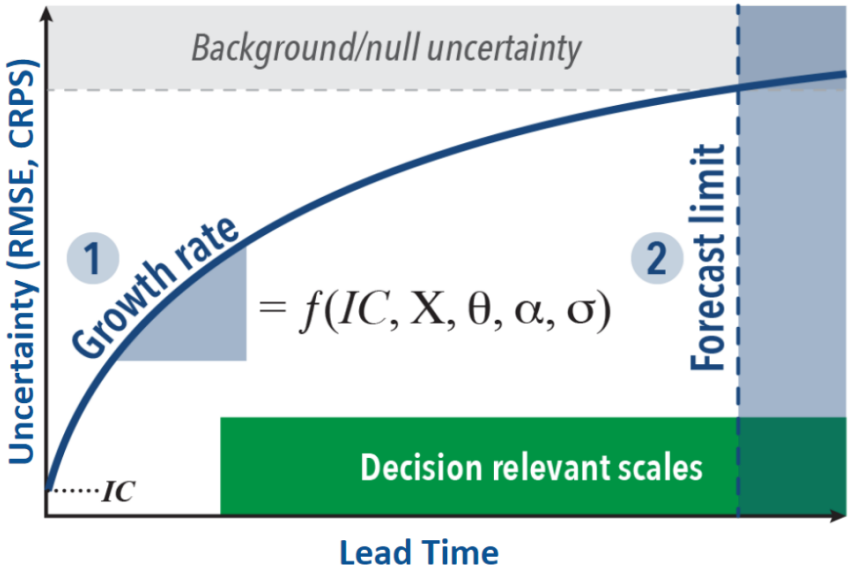


Figure 1: Conceptual diagram of a modeled state uncertainty (y-axis) against time/space (x-axis) whereby the modeled state is a result of function using initial conditions and other parameters. Growth rate is the slope of the function and forecast limit is the intersection of the function with null uncertainty (random chance).

Previous studies on the theory of predictability for ecosystem states call for clear quantitative analyses on verifiable forecasts in order to create a systematic understanding of predictability (Dietze, 2017a; Luo et al., 2015). This reasoning borrows from the major advancements made in the realm of weather forecasting over the past 100 years (Smagorjnsky, 1983). Numerical weather forecasts began as daily predictions using yesterday's observations to predict tomorrow's state; with the data boom over the past 40 years these predictions have become more accurate (Bauer et al., 2015). Satellite and tower measurements of conditions improved weather forecast skill using data assimilation (Leith, 1974; Zhang, Hailing. Pu, Zhaoxia, 2010). The weather forecast skill, as a function of forecast lead time, has improved at a rate of 1 day per decade; so our current 6-day forecast is as accurate as the 5-day forecast a decade ago (Bauer et al.,

2015). In addition to providing societally-useful predictions, weather forecasts embody our hypotheses about how the atmosphere works, and the daily validation of these predictions has helped improve future weather forecasts, slowly closing the gap between model predictions and observations (Dietze et al., 2018). The current success and dependability of weather forecasts provides a model that carbon cycle scientists might emulate to improve our ecological forecasts and investigate the predictability of terrestrial carbon and water cycles.

The study of predictability goes beyond simply assessing model skill. One way to understand predictability is to determine the rate at which uncertainty in a prediction increases as a function of forecast lead time (Figure 1, growth rate) (Dietze, 2017a). The uncertainty growth rate is a function of the uncertainty and sensitivity in the model initial conditions, meteorological drivers, parameters, and other exogenous factors. The use of iterative near-term ecological forecasts over time should result in more consistent and accurate predictions of ecosystems (Dietze et al., 2018; White et al., 2019). Iterative forecasting refers to the process of updating predictions when new observations become available; thereby mimicking the real-time cycling of elements through an ecosystem (Dietze, 2017a). By continually confronting predictions with new observations, near-term iterative forecasting allows us to test hypotheses and close the gap between ecosystem models and observations (Dietze, 2017b). Near-term forecasts operate on the daily to decadal timescales that are relevant for land management decisions; examples include daily forecasts for tracking toxic algal blooms to decadal forecasts tracking bird biodiversity (Dietze, 2017b; Stumpf et al., 2009; White et al., 2019). As a prototype

workflow to begin investigating the predictability of carbon and water cycles, here I report on the development and assessment of a 35-day iterative forecast of the terrestrial carbon and water cycles.

While this forecasting workflow could be used to study changes to carbon and water cycles across a myriad of ecosystem types and locations, for this initial proof-of-concept the workflow is applied to one site, Harvard Forest, a temperate deciduous forest in the Northeastern United States. This region is well-studied, and this study site is particularly data rich and frequently used for model calibration and validation. Harvard Forest is an ideal testbed for developing an automated forecasting workflow and addressing some initial questions about terrestrial ecosystem predictability. Given the near-term focus of the forecast, and existing data availability, I focus on the predictability of carbon stores with short residence times (e.g., leaf carbon), as well as the net carbon and water fluxes as proxies for their overall cycles. In particular, I focus on Net Ecosystem Exchange of CO2 (NEE) and the latent energy (LE) flux between the land and atmosphere as these are routinely measured at many sites using eddy covariance and vary on diurnal, synoptic, and seasonal timescales (Pastorello et al., 2020). I focused on remotely-sensed leaf area index (LAI) as a proxy for the leaf carbon store to match the sub-seasonal timescale of the forecast.

Our primary research question is: **What is the near-term predictability of terrestrial pools and fluxes (NEE, LE, LAI)?** Furthermore, how is the predictability of terrestrial pools and fluxes improved by the iterative assimilation of NEE, LE, and LAI observations? Our hypotheses are as follows:

1. Terrestrial pools and fluxes are most predictable the first week after the forecast is made and gets less predictable as the forecast horizon increases. Most near-term weather forecasts are most predictable the first week, so our predictions should behave similarly (Lynch, 2008; Thompson, 1957). Quantitatively, this means that the uncertainty (figure 1) will rapidly increase over the first week and then level off over the following weeks.
2. Leaf carbon stores are more predictable than terrestrial fluxes. Leaf carbon stores undergo a seasonal turnover while terrestrial fluxes operate on a diurnal cycle, therefore if the carbon remains in the ecosystem longer (i.e., longer residence time) it will be easier to predict (Bonan, Gordon, 2016; Byrne et al., 2020; Hicke et al., 2002). Quantitatively, the forecast limit (figure 1) will occur sooner in the forecast for terrestrial fluxes than for leaf carbon stores.
3. Assimilation of observations will improve prediction accuracy of terrestrial pools and fluxes compared to unconstrained predictions. Including observations as constraints will give the model a better starting point for predictions, and the assimilation of MODIS LAI has been shown to improve model precision and accuracy (Baldocchi et al., 2018; Dokoohaki et al., 2021; Tian et al., 2022; Zeng et al., 2008). Quantitatively, this means that the y-intercept of the unconstrained predictions will be greater than that of the predictions constrained with observations.

## Methods

State Data Assimilation (SDA) & Iterative Forecasting Workflow

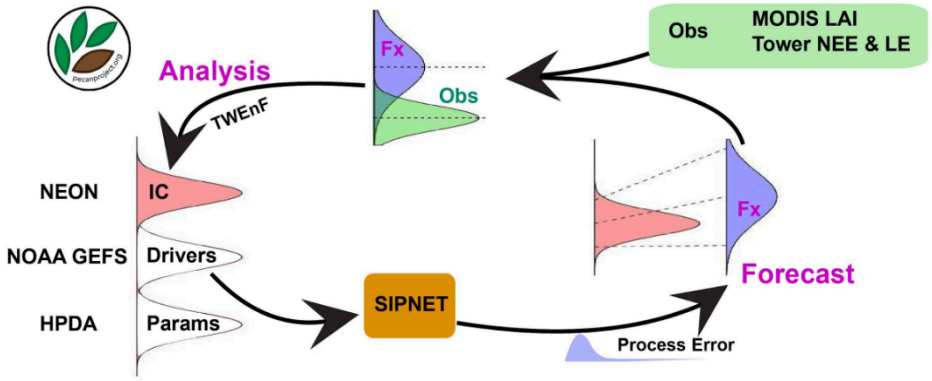


Figure 2: Conceptual Diagram of Iterative Forecasting Workflow: t=1 uses NEON IC, t=n uses predictions from previous forecast day. National Ecological Observatory Network (NEON), National Oceanic and Atmospheric Administration (NOAA) Global Ensemble Forecast System (GEFS), Hierarchical Bayesian Data Assimilation (HPDA), Tobit-Wishart Ensemble Filter (TWEnF), Forecast (Fx), Observations (Obs), Initial Conditions (IC), Parameters (Params).

I developed the forecasting workflow within the Predictive Ecosystem Analyzer (PEcAn) ecological data-informatics system (Cowdery et al., 2014; D. LeBauer et al., 2018; D. S. LeBauer et al., 2012/2013). This open-source community cyberinfrastructure comes equipped with functions for processing model inputs and outputs, running ecosystem models, and analyzing model output (Figure 2). All code used for this research is available in the PEcAn repository on Github (https://github.com/PecanProject/pecan, version 1.7.2). The PEcAn platform includes a centralized database, BETY, which catalogs all of the model inputs and outputs along with site specific information related to species composition. This community cyberinfrastructure platform reduces the amount of

redundant model input processing work, helps support reproducibility, and supports the advancement of the field as a whole as data ecological data volumes increase (Fer, Gardella, et al., 2021).

The forecast system employs a State Data Assimilation (SDA) framework to iteratively update the carbon and water cycle state variables as part of a forecast-analysis cycle (Figure 2). In the forecast step, the ensemble-based forecasting approach was used to make a probabilistic forecast over the next 35-days. As part of the analysis step, I statistically reconcile the difference between these predictions and the new observations that have accumulated over that period (Figure 2b). Ensemble-based SDA takes a Bayesian approach to the analysis step, with the forecast providing an informative prior constructed by fitting a known probability distribution to the ensemble predictions. The forecast priors are updated through a statistical Likelihood to generate posterior distributions of the system state variables (in this case carbon and water pools) that then serve as initial conditions for the next forecast. Within the statistical Likelihood the probability that any forecast produced the observed data is calculated based on the reported observation error in the data product, with any additional discrepancy between model and data attributed to process error.

There are numerous ensemble-based SDA techniques available and for this analysis the Tobit-Wishart Ensemble Filter (TWEnF) was implemented as part of the PEcAn (Predictive Ecosystem Analyzer) model-data informatic system (Fer, Shiklomanov, et al., 2021; Raiho et al., 2020). The TWEnF has two key advantages when it comes to assimilating ecological data. First, the analysis allows the use of a Tobit

distribution, which is a zero-truncated and zero-inflated version of the Normal distribution, as both the forecast prior and analysis Likelihood. Here specifically I used the Tobit censoring in the assimilation of MODIS LAI data, while using the more conventional Normal prior and Likelihood to assimilate NEE and LE. The second advantage of the TWEnF is that it enables us to sequentially update our estimate of the model's process error, rather than treating this as known *a priori*. A Wishart prior is used to allow the estimation of the full process error covariance matrix, thus quantifying (and propagating) both the model's residual uncertainty in its predictions (in this case, LAI, NEE, and LE) and the correlations (across pools and fluxes) in these errors. See Raiho et al. (2020) for a full description of the framework.

The workflow was configured to assimilate LAI, NEE, and LE at a daily time step. One of the powerful features of SDA is that it allows you to not only update the pools and fluxes you observed, but also those that were unobserved, which are constrained indirectly based on the covariances in the forecast (prior) between observed and unobserved variables. Thus, the output of the analysis step is an updated estimate of aboveground wood carbon, leaf carbon (LAI), soil moisture, and soil carbon. This feature of indirect updating allows SDA to easily handle missing data for any of the data constraints. Most data sources can be used for validation of model output however for data to be used for assimilation I need an estimate of uncertainty. These uncertainty estimates help the workflow evaluate the confidence in each observation. If data constraints are missing on a particular day, then the SDA is not run, and that day's forecast uses the previous forecast as initial conditions.

Site & Data Description

Harvard Forest is located in central Massachusetts (42.5° N, 72.2° W) and is a secondary forest primarily composed of red oak (Quercus rubra), eastern hemlock (Tsuga canadensis), and red maple (A. rubrum) (Finzi et al., 2020). Harvard Forest was established as a research site in 1907 and in addition to being the longest running Ameriflux site, is also a member of the LTER, NEON, and ForestGEO networks. The abundance of data makes this site the ideal test case for our daily forecasting workflow.

The forecast workflow ran from September 2020-December 2021 using the NOAA GEFS (Global Ensemble Forecast System) weather forecast as meteorological drivers (NOAA, n.d.-c). The 35-day ensemble member forecast first became available September 2020. From GEFS I extracted the following meteorological drivers: air temperature, precipitation, short wave (solar) radiation, humidity, and wind speed. GEFS generates a 31-member ensemble which was resampled with replacement as drivers to the 100 model ensemble members.

Initial condition estimation

Estimated initial conditions for the SIPNET carbon pools used NEON plot survey data collected in 2019. I leveraged the annual biomass plot surveys to initialize the wood and leaf carbon pools using allometric function of diameter at breast height (DBH) to predict total biomass and leaf biomass (*NEON | Herbaceous Clip Harvest*, n.d.; *NEON | Plant Presence and Percent Cover*, n.d.; *NEON | Vegetation Structure*, n.d.). The initial condition ensemble members were created by statistically resampling the NEON vegetation survey data. I separated out the collected data into plots (woody vegetation)

and subplots (herbaceous vegetation) based on the NEON designations and then resampled within those groups. The soil carbon initial condition ensemble members were generated with soil bulk density and soil C measurements collected from the initial 2012 NEON megapits, but due to the low replication in this data I was not able to create ensemble members (*NEON | Soil Physical and Chemical Properties, Megapit*, n.d.).

Posterior parameter distributions for SIPNET's temperate deciduous plant functional type (PFT) come from Fer et al. (2018, 2021), who used an emulated Hierarchical Bayesian approach to calibrate the model against eddy-covariance data from 12 temperate deciduous Ameriflux sites (Fer et al. 2018, 2021). Parameter vectors for individual ensemble members were sampled from the joint posterior distribution, which accounts for parameter covariances.

Observations

For LAI observations, I relied on the Moderate Resolution Imaging Spectrometer (MODIS) MOD15A2H 8-day, 500m composite product. The algorithm chooses the best pixel over the 8-day period and reports a quality control value along with observation error (Myneni,  Ranga et al., 2015). I accessed the MODIS data via the MODISTools R package (Hufkens & Labs, 2023).

For NEE and LE I assimilated eddy-covariance tower observations taken from the Harvard Forest Environmental Monitoring Station (EMS) tower (cite). The U* filtering and gap-filling were performed using the OneFlux data product (Pastorello et al., 2020). Because the assimilation is only performed once a day, 30-minute measurements were aggregated to daily averages along with an estimate of observation error.

SIPNET model

The Simplified Photosynthesis and Evapotranspiration model (SIPNET) is a process-based carbon and water flux ecosystem model designed for comparison to eddy-flux data (Braswell et al., 2005; Zobitz et al., 2008). The model has been successfully calibrated and validated against eddy covariance NEE and LE observations across a range of temperate deciduous and conifer forest sites (Dokoohaki et al., 2021; Fer et al., 2018; Fer, Shiklomanov, et al., 2021; Moore et al., 2008). More recently the SIPNET model was used in the development of a continental-scale carbon cycle reanalysis product across the continuous U.S. constrained by MODIS LAI and a LANDSAT-based aboveground biomass product (Dokoohaki et al., 2021).

SIPNET contains three primary carbon stores or pools: wood carbon (woodC), leaf carbon (leafC), and soil carbon (soilC); and models the flow to carbon among these three pools and between the land and the atmosphere (Braswell et al., 2005). Gross primary productivity (GPP) is modeled using a light use efficiency approach, with additional environmental constraints from air temperature, soil moisture, and VPD (Braswell et al., 2005). Heterotrophic respiration is modeled as a function of soil carbon content and soil moisture (Braswell et al., 2005). Autotrophic respiration (Ra) is the sum of foliar maintenance respiration and wood maintenance respiration, each of which is proportional to pool size (Braswell et al., 2005). SIPNET assumes leaf and wood allocation are constant fractions of Net Primary Productivity (NPP = GPP - Ra) and that leaf and wood turnover rates are constant over time (Braswell et al., 2005). SIPNET's leaf phenology is based on prescribed phenological transition dates; over the course of

one timestep all leaves in the model will appear and disappear. LAI is calculated as

$$LAI = leafC/SLA, \quad \text{Eq.1}$$

where SLA is the specific leaf area.

SIPNET also contains water pools for soil moisture, litter moisture, and snow (Sacks et al., 2006). Evapotranspiration is calculated as

$$ET = Ei + Ep + Es + T, \quad \text{Eq.2}$$

where Ei is canopy interception, Ep is sublimation, Es is soil evaporation, and T is transpiration. Interception is modeled as a constant fraction of precipitation and is immediately evaporated during that time step. Evaporation is modeled as a function of vapor pressure deficit (VPD) and soil VPD, with canopy and soil resistance modeled as functions of wind speed and soil moisture, respectively. Sublimation is modeled using vapor pressure and available snow. Transpiration is split into two scenarios: water saturated and water stressed; in the water saturated case transpiration is equal to potential transpiration calculated as GPP/WUE while in the water stressed case transpiration is calculated using a soil water availability parameter applied to potential transpiration (Aber & Federer, 1992). To convert evapotranspiration into latent heat flux (LE) I multiplied the output by the latent heat of vaporization of water.

Uncertainties in the SIPNET forecasts are propagated using an ensemble-based approach that varies the model parameters, meteorological drivers, and initial conditions (Dietze, 2017a). Similar model experiments use 20 or fewer ensemble members, but some have concluded that this might be too few to properly represent the uncertainty

(Cranko Page et al., 2022; Dokoohaki et al., 2021; Zeng et al., 2008). For this analysis I chose to increase the ensemble size to 100; further descriptions of how each input ensemble is generated can be found in the data section.

Analysis

Using the described forecasting workflow, I ran two experiments: unconstrained runs and MODIS LAI constrained runs. I used the output of all experiments to evaluate my hypotheses focused on predictability and compare the output across experiments to evaluate our hypotheses on data assimilation.

My primary research question "What is the near-term predictability of terrestrial pools and fluxes?" relies on a well-understood definition of predictability. Predictability is the change in uncertainty over time or space; in this case we are measuring the uncertainty over a 35-day period. For this analysis I used four methods for estimating uncertainty: root mean squared error (RMSE), mean absolute error (MAE), bias, and continuous ranked probability score (CRPS). RMSE is calculated as:

$$RMSE = \sqrt{\frac{1}{n}\sum_{i=1}^{n}(x_i - y_i)^2} \qquad \text{Eq.3}$$

MAE is calculated as:

$$MAE = \frac{1}{n}\sum_{i=1}^{n}|x_i - y_i| \qquad \text{Eq.4}$$

Bias is calculated as:

$$bias = \sum_{i=1}^{n} x_i - y_i \text{Eq.5}$$

CRPS is calculated as:

$$CRPS(CDF, y) = \sum_{i=1}^{n} u_i |x_i - y| - \frac{1}{2} \sum_{i,j=1}^{n} u_i u_j |x_i - x_j| \quad \text{Eq.6}$$

Where in the above equations *n* is the number of predictions, *x* is the prediction, and *y* is the observation. The *u* variables are nonnegative and sum to 1 and are used to weight the equation, in this case I used the crps_sample function from the scoringRules package which defaults to equally weight the equations (i.e., u = 1/n) (Jordan et al., 2020).The RMSE, MAE, and Bias calculations compare the daily average of our predictions (NEE, LE & LAI) to the daily average of the observations, while the CRPS calculation leverages information across ensemble members to compare a prediction distribution to an observation. RMSE helps to understand how much spread exists in the errors, so a lower RMSE value indicates less error spread among predictions. The bias score should provide information on systematic model error (i.e. underestimating or overestimating predictions). Typically, RMSE and bias are viewed together to indicate what the error spread is and in what direction (positive or negative) the error trend.

$$RMSE = \sqrt{bias^2 + var} \quad \text{Eq. 8}$$

RMSE can be decomposed into bias and variance (Eq. 8). Bias and variance are inversely connected, so the total RMSE can be parsed out between bias and variance. CRPS compares an observation to the cumulative distribution function (CDF) of the predictions. If the workflow ran without ensemble members, then the CRPS and MAE would be the same value, so the comparison of these two metrics gives insight to the impact of ensemble spread on prediction error. To compare across datasets to evaluate our second hypothesis I calculated a normalized RMSE (NRMSE) by dividing RMSE by the mean

observation (NEE, LE, LAI).

I am not assuming that the relationship between the uncertainty metrics and lead time is linear, so I am employing generalized additive models (GAMs) to parse out the underlying trends using the R mgcv package (Wood, 2022) called from R (R Core Team, 2023; Version 4.2.1). The GAMs method used restricted maximum likelihood (REML) with the default number of knots (n=10). I calculated the GAMs for each of the uncertainty metrics (RMSE, bias, CRPS, MAE) versus forecast lead time.

I calculated the predictive interval (PI) for an example forecast using the 95th quantiles across ensemble members of the daily mean for each variable (NEE, LE, and LAI). To illustrate the impact of assimilation on the forecasts, I visualized the June 2, 2021 forecast since this forecast includes a MODIS LAI observation available for assimilation. All intermediate model output and analyses are stored on the Boston University Department of Earth and Environment shared computing cluster with finalized forecast output on GitHub (https://github.com/helge22a/SIPNET-SDALAI-Thesis).

## Results

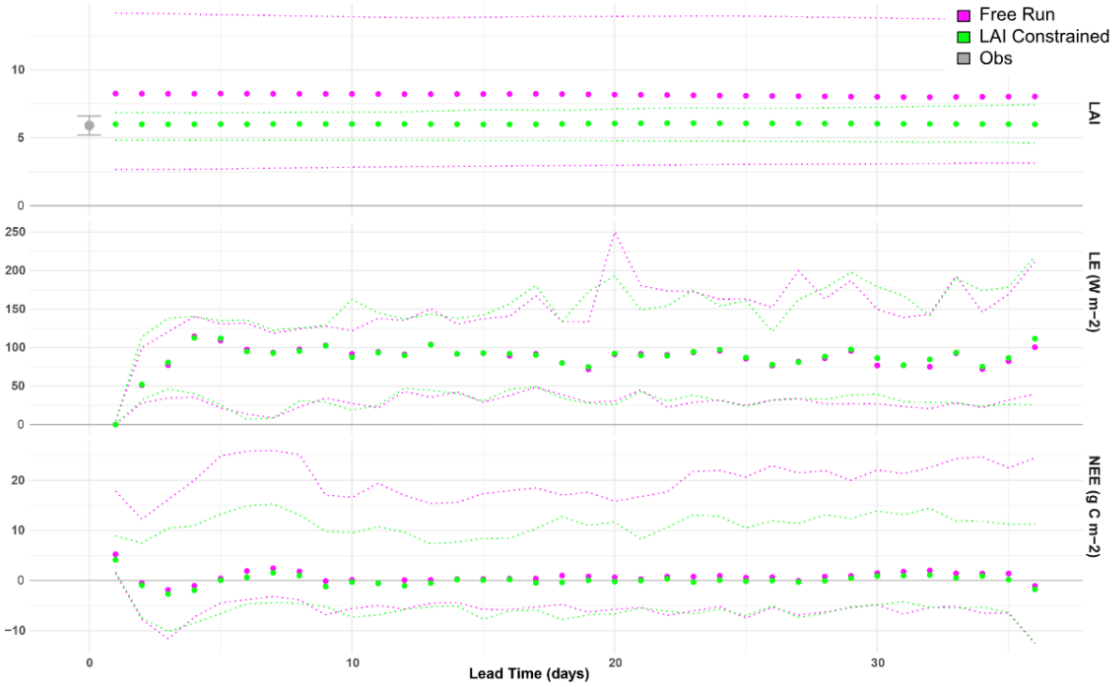


Figure 3: Example forecast with assimilation of MODIS LAI observation for start date of 2021-06-02 of LAI, LE, and NEE with 95% PI (dotted).

Every day from September 29, 2020 to December 31, 2021 a 35-day forecast ran with 100 ensemble members. Over the 2021 growing season MODIS LAI observations were assimilated that passed qc check. The forecast made on June 2, 2021 ran with model states updated with a MODIS LAI observation of 5.9. There is a clear and immediate reduction in LAI comparing the unconstrained forecast to the MODIS LAI constrained forecast (Figure 3). The PI interval shrinks for LAI when an observation is included for assimilation (Figure 3). There does not appear to be a large shift in predictions of LE when a MODIS LAI observation is assimilated (Figure 3). The predictions of LE increase over the first 3 days of the forecast and then reach a plateau (Figure 3). Similarly, there is a decrease in NEE over the first 3 days of the forecast (Figure 3). There is a slight

decrease in NEE when a MODIS LAI observation is assimilated (Figure 3).

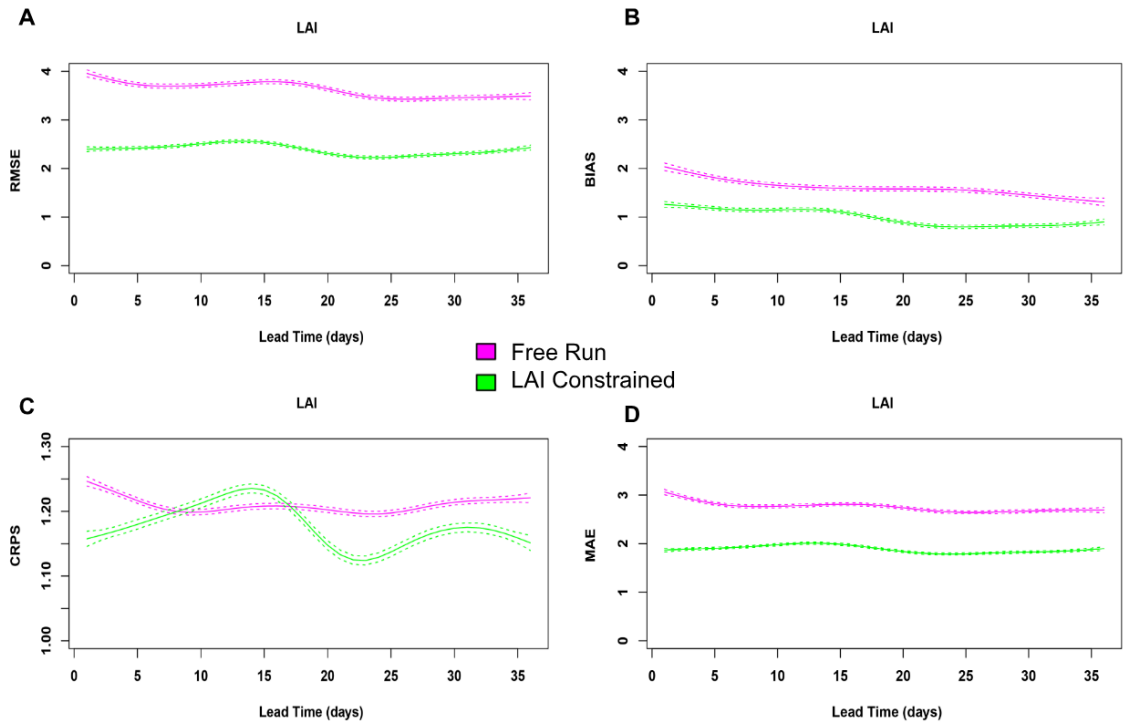


Figure 4a: RMSE with GAM on Lead Time for MODIS LAI constrained predictions of LAI and unconstrained predictions of LE; DOY filtered to match. Figure 4b: Bias with GAM on Lead Time for MODIS LAI constrained predictions of LAI and unconstrained predictions of LE; DOY filtered to match. Figure 4c: CRPS with GAM on Lead Time for MODIS LAI constrained predictions of LAI and unconstrained predictions of LE; DOY filtered to match. Figure 4d: MAE with GAM on Lead Time for MODIS LAI constrained predictions of LAI and unconstrained predictions of LE; DOY filtered to match.

Some predictions were most accurate within the first week and others were less accurate. For LAI the lowest RMSE score occurs at a lead time of 20 days for unconstrained predictions and at a lead time of 24 days for MODIS LAI constrained predictions (Figure 4a). Similar trends in the Bias and MAE scores were observed. The lowest value was around a lead time of 20 days for unconstrained predictions and around a lead time of 24 days for MODIS LAI constrained predictions of LAI (Figure 4b,d). The CRPS trend across lead time for unconstrained predictions of LAI appears almost as a

straight line with no clear minimum, while the CRPS trend for MODIS LAI constrained predictions of LAI also shows a minimum value around a lead time of 24 days similar to the trends observed in the RMSE, Bias, and MAE scores (Figure 4b).

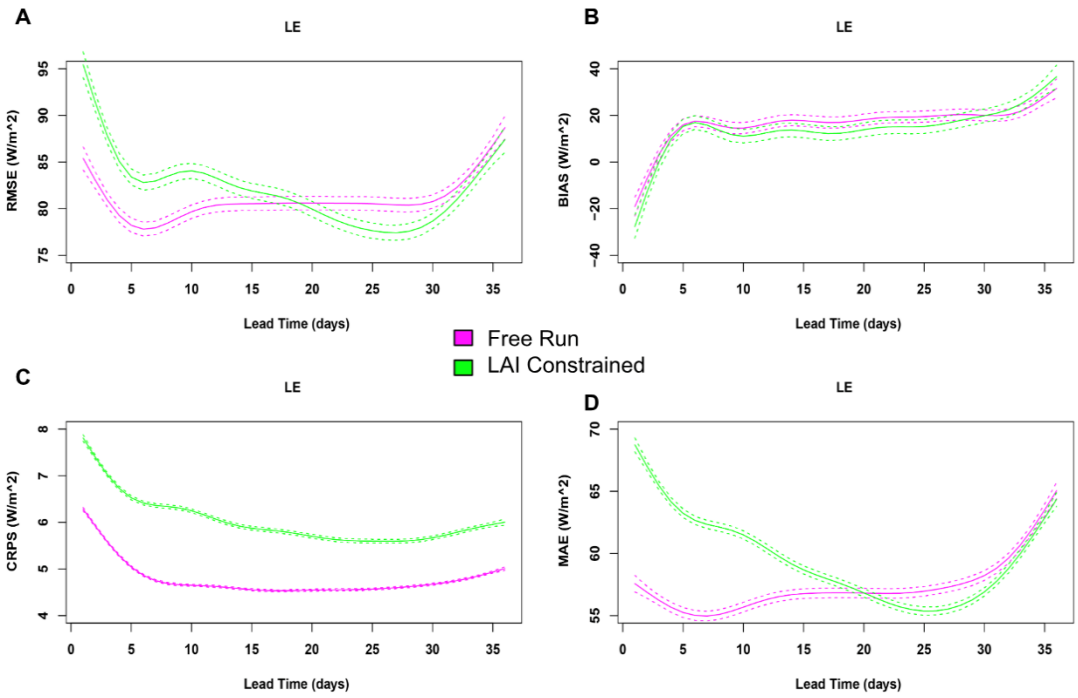


Figure 5a: RMSE with GAM on Lead Time for MODIS LAI constrained predictions of LE and unconstrained predictions of LE; DOY filtered to match. Figure 5b: Bias with GAM on Lead Time for MODIS LAI constrained predictions of LE and unconstrained predictions of LE; DOY filtered to match. Figure 5c: CRPS with GAM on Lead Time for MODIS LAI constrained predictions of LE and unconstrained predictions of LE; DOY filtered to match. Figure 5d: MAE with GAM on Lead Time for MODIS LAI constrained predictions of LE and unconstrained predictions of LE; DOY filtered to match.

The RMSE, CRPS, and MAE trends across lead time for predictions of LE followed a parabola shape while the Bias score follows a more sigmoidal shape (Figure 5). The lowest RMSE and MAE scores occurred at a lead time of 5 days for unconstrained predictions of LE and at a lead time of 25 days for MODIS LAI constrained predictions of LE (Figure 5a,d). The CRPS minimum for both experiments occurred around a lead time of 5 days (Figure 5c). The bias began at a lead time of 0 days

as a negative value and then reached the zero line at day 5 and remained positive for the remainder of the forecast period (Figure 5b). The CRPS and bias results provided support for the first hypothesis; that the lowest uncertainty value should occur within the first 7 days of the prediction.

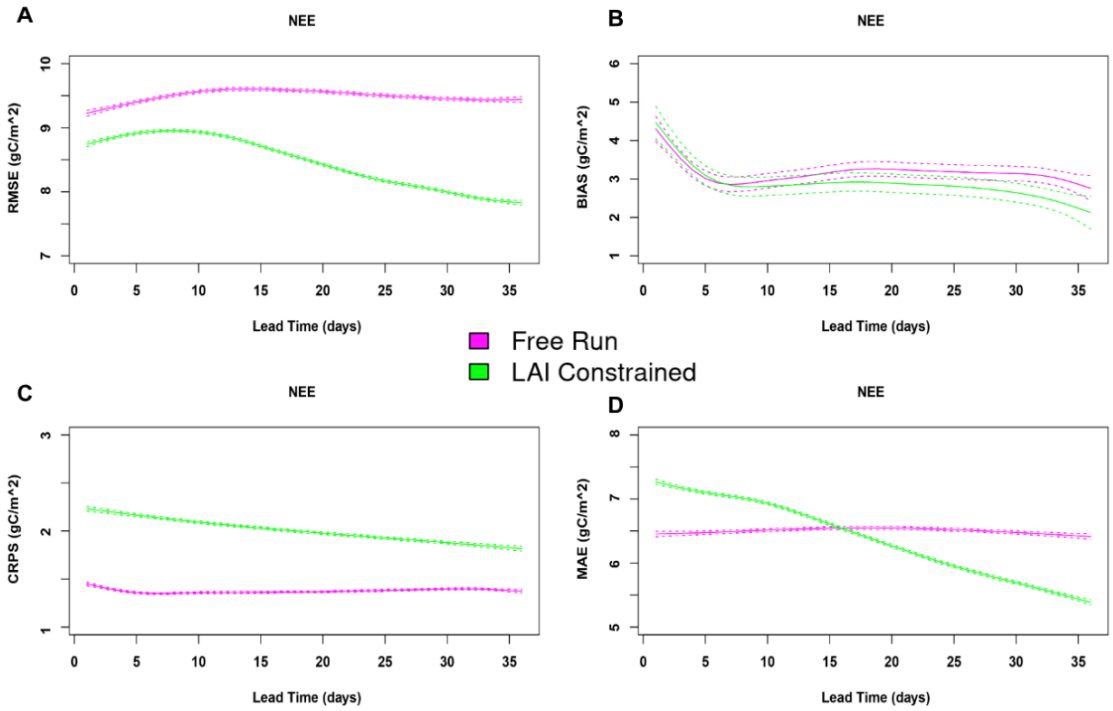


Figure 6a: RMSE with GAM on Lead Time for MODIS LAI constrained predictions of NEE and unconstrained predictions of NEE; DOY filtered to match. Figure 6b: Bias with GAM on Lead Time for MODIS LAI constrained predictions of NEE and unconstrained predictions of NEE; DOY filtered to match. Figure 6c: CRPS with GAM on Lead Time for MODIS LAI constrained predictions of NEE and unconstrained predictions of NEE; DOY filtered to match. Figure 6d: MAE with GAM on Lead Time for MODIS LAI constrained predictions of NEE and unconstrained predictions of NEE; DOY filtered to match.

The greatest disagreement between uncertainty metrics was for NEE. The lowest RMSE score occurs at a lead time of 0 days for unconstrained predictions of NEE and at a lead time of 35 days for MODIS LAI constrained predictions of NEE (Figure 6a). The lowest Bias score occurred at a lead time of 35 days across both experiments (Figure 6b). The CRPS trend appeared to follow a straight line across lead time for both experiments

(Figure 6c). While the MAE trend for unconstrained predictions of NEE followed a similar pattern to the CRPS trend, the MAE for MODIS LAI constrained predictions of NEE showed a negative linear trend across lead time (Figure 6d).

I observed clear support for the second hypothesis, that leaf carbon stores were more predictable than terrestrial fluxes. Comparing the predictability across all three variables I observed that LAI was the most predictable with a NRMSE of ~1.4% for unconstrained predictions (Figure 7). LE is the second most predictable with a NRMSE of ~2% for unconstrained predictions (Figure 7). NEE is by far the least predictable with a NRMSE of ~18% for unconstrained predictions (Figure 7).

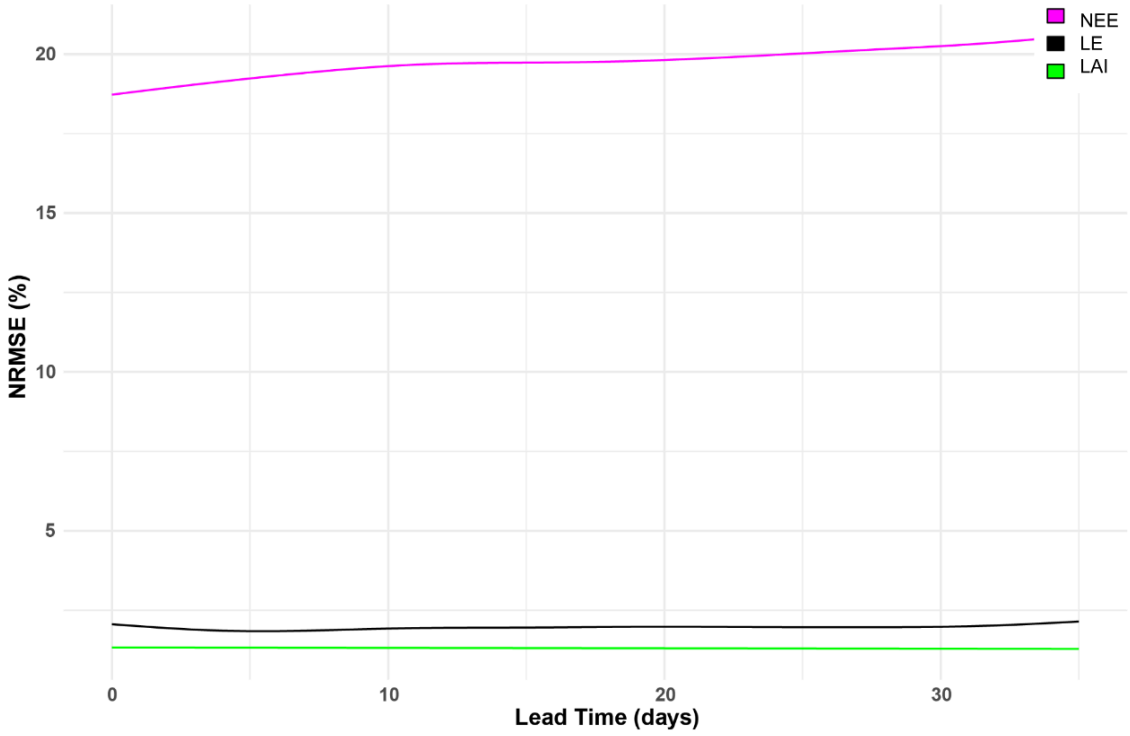


Figure 7: Comparison of unconstrained NRMSE across LAI, LE & NEE.

The third hypothesis was supported as the assimilation of observations decreased uncertainty over lead time. When MODIS LAI observations were assimilated, the RMSE decreased by ~50% compared to unconstrained predictions of LAI (Figure 4a). A similar trend was observed in the bias and MAE scores comparing MODIS LAI constrained predictions of LAI to unconstrained predictions of LAI (Figure 4b,d). The CRPS trend for MODIS LAI constrained predictions passed the unconstrained predictions around a lead time of 14 days (Figure 4c). However, this trend is short lived and only lasts approximately 3 days before the MODIS LAI constrained predictions of LAI dropped below the unconstrained predictions of LAI (Figure 4c).

There was a lag in the improvement of uncertainty for LE. The RMSE and MAE of the MODIS LAI constrained predictions of LE dropped below the unconstrained predictions of LE after two weeks (Figure 5a, d). Furthermore, the Bias score showed no clear distinction between the two experiments (Figure 5b). Contradicting the RMSE and MAE trends, the CRPS for MODIS LAI constrained predictions of LE increased by ~1.3% compared to unconstrained predictions of LE (Figure 5c).

The uncertainty metrics disagree on the magnitude of improvement for predictions of NEE across lead time. There was a decrease in RMSE of ~10% of MODIS LAI constrained predictions compared to unconstrained predictions (Figure 6a). Similar to LE, the Bias metric did not distinguish between the two experiments and the CRPS increased for MODIS LAI constrained predictions of LE compared to unconstrained predictions of LE (Figure 6b, c). There was a decrease in MAE after the first two weeks when for the MODIS LAI constrained predictions of LE compared to the unconstrained

predictions of LE (Figure 6d).

**Discussion**

I set out with two goals, to create a prototype iterative near-term forecasting workflow of the carbon and water cycles, and to use this forecast to better understand the inherent predictability of carbon and water stores and fluxes. Unlike many other forecasts, the terrestrial carbon and water cycle forecast was not necessarily more accurate closer to the forecast date. While the uncertainty of LAI, NEE, and LE was expected to be positively correlated with forecast lead time, there was variability in the result depending on the uncertainty metric used. Some variables showed a negative linear relationship with lead time and others showed a non-linear relationship between uncertainty and forecast lead time. Both LE and NEE predictions varied the most during the first three days of the forecast, so the initial high uncertainty values could be the result of model transience. This was the first study to use a weather forecast as the meteorological driver and include MODIS LAI for assimilation in an investigation on the inherent predictability of LAI, NEE, and LE, therefore there were no direct result comparisons to make in the analysis of uncertainty over forecast lead time.

There was a lag in the improvement of LE uncertainty when I assimilated MODIS LAI observations. While both experiments reported negative Bias values within the first 5 days; these results are for separate but related reasons: 1) decrease in transpiration, and 2) mis-calibrated model parameters. LE represents the exchange of water between the land and atmosphere, and one of the major components driving this exchange is the amount of leaves present. I observed that the assimilation of MODIS LAI observations

improved prediction accuracy of LAI by ~50%. So when I used the assimilation, day 1 LAI was a realistic representation of the amount of leaves present and therefore available for transpiration. In general, when I assimilated LAI observations the day 1 LAI decreased compared to unconstrained predictions, therefore the model transpiration decreased leading to an overall decline in LE.

Unlike for LE, the four uncertainty metrics cannot agree on the shape of NEE uncertainty over forecast lead time. The NRMSE result supports the conclusion that LE is more predictable than NEE, but these fluxes do follow similar trends. Similar to the lag in LE, there was a two-week lag in improvement of NEE predictability after assimilating MODIS LAI observations. NEE is the exchange of carbon between the land and atmosphere, and LAI sets the leaf carbon pool size in our workflow. Unlike LE, where a decrease in LAI leads to an underestimation of LE, the NEE bias results suggest that a decrease in LAI leads to an overestimation of NEE. Two out of the four uncertainty metrics support that the assimilation of MODIS LAI decreases NEE uncertainty over lead time. These results suggest a need to re-parameterize some of the carbon cycle parameters.

A re-analysis study using MODIS LAI for assimilation reported a reduction in uncertainty in NEE after assimilation, but this study relied on the post-hoc ensemble adjustment for NEE (Dokoohaki et al., 2021). Other studies evaluating the impact of LAI observations on NEE occurred over a longer time period and the associated analyses focused on aggregated weekly NEE (Dokoohaki et al., 2021). Similar model experiments investigating the impact of assimilating LAI observations on the “predictability” of latent

heat flux did not see an improvement in predictions of LE until 60 days, which falls outside the range of our 35 day forecast (Tian et al., 2022). This study also reports comparable uncertainty ranges for their “predictions" of LE to our RMSE values (Tian et al., 2022).

The forecasting workflow updates all model states at the beginning of each new forecast using the previous day's model output; if a MODIS LAI observation is available then the data is assimilated and used to inform the next day’s model states. Fluxes are not model states, so the fluxes themselves are never directly informed by a MODIS LAI observation. Instead, the MODIS LAI assimilation impacts subsequent NEE predictions via the updated leaf, wood, and soil carbon stores and LE via the updated LAI and soil moisture, with wood C, soil C, and soil moisture updated indirectly through the covariation of LAI with these model states. This workflow does not use assimilation to update any model parameters; so while the MODIS LAI observation nudges the model states towards reality it is likely that parameter errors could be causing the calculation of the fluxes to be off. Specifically, the model parameters related to autotrophic respiration are likely causing total ecosystem respiration to be too high. This causes the growing season NEE to be positive (i.e., more carbon respired than stored) rather than negative.

Carbon cycle calibration studies rely on updating model parameters as opposed to model states; one such study used in situ flux measurements and satellite FAPAR to update carbon fixation, respiration, and phenology parameters did see an improvement in model-data agreement (Bacour et al., 2015). Another study assimilating LAI and soil moisture data to inform model parameters observed the greatest improvement in flux

predictions after assimilating both data streams (Albergel et al., 2010). More recent studies also found an improvement in GPP prediction with the assimilation of soil moisture data (Xing et al., 2023). These results are in line with experimental studies that track the variation in GPP by latitude and attribute the variation to differences in soil moisture (Baldocchi et al., 2018).

This research set out to test the prototype forecasting and data assimilation workflow using one site and one data constraint, but if we want to understand the inherent predictability of the terrestrial carbon and water cycles we need to include more sites and more data constraints in future experiments. Increasing the number of sites allows us to analyze the spatial variability of predictability, while increasing the number of data constraints allows us to decrease the uncertainty associated with the predictions. Future model experiments should include additional near-term data streams as part of the data assimilation, such as soil moisture, eddy-co flux measurements, and soil respiration. This research also relied on a single mesic forest ecosystem. By running the forecast workflow across a range of ecoregions we would be able to determine if terrestrial carbon and water cycle predictability varies by region; for example, are mesic ecosystems easier to predict than arid ecosystems? In addition to exploring the spatial variability of predictability, future experiments should explore the temporal variability of predictability by running the workflow with longer forecast time series. The results do not show a change in predictability of LAI at the 35-day time scale, but a seasonal forecast may show greater temporal variation in predictability. A longer forecast time series would also be better suited to analyzing the predictability of slower changing carbon stores (wood,

soil). Suitable meteorological forecasts to use as inputs include the Climate Forecast System (CFS) (NOAA, n.d.-b) with a 9-month forecast horizon or the North American Multi-Model Ensemble forecast with a 3-month forecast horizon (NOAA, n.d.-a).

**Conclusions**

If we understand how terrestrial carbon and water cycle predictability varies spatially and temporally, then we can better inform global land models and data collection efforts. We can focus resources on regions with higher predictive uncertainty to try and reduce the uncertainty through data collection efforts. This initial research concluded that uncertainty in LAI, LE, and NEE was not positively correlated with forecast lead time, the assimilation of MODIS LAI observations improved predictability of LAI, LE, and NEE, and LAI was more predictable than LE or NEE at a temperate deciduous forest in Northeastern U.S. This single-site experiment using the prototype forecasting workflow contained unrealistic NEE predictions caused by model miscalibration, which illustrates a challenge with scaling up forecasts to more broad regional scales where such ground validation data is not available for every site being forecast. Identifying the errors at this scale makes it easier to fix and then scale-up the experiment once the errors are fixed. Over time the use of iterative forecasting workflows will improve our ability to make predictions about the future state of ecosystems, but it is important to be realistic about current forecast skill and the time and energy required for iterative forecast refinement.

## References

Aber, J. D., & Federer, C. A. (1992). A generalized, lumped-parameter model of photosynthesis, evapotranspiration and net primary production in temperate and boreal forest ecosystems. *Oecologia*, *92*(4), 463–474. https://doi.org/10.1007/BF00317837

Albergel, C., Calvet, J.-C., Mahfouf, J.-F., Rüdiger, C., Barbu, A. L., Lafont, S., Roujean, J.-L., Walker, J. P., Crapeau, M., & Wigneron, J.-P. (2010). Monitoring of water and carbon fluxes using a land data assimilation system: A case study for southwestern France. *Hydrology and Earth System Sciences*, *14*(6), 1109–1124. https://doi.org/10.5194/hess-14-1109-2010

Bacour, C., Peylin, P., MacBean, N., Rayner, P., Delage, F., Chevallier, F., Weiss, M., Demarty, J., Santaren, D., Baret, F., Berveiller, D., Dufrene, E., & Prunet, P. (2015). Joint assimilation of eddy covariance flux measurements and FAPAR products over temperate forests within a process-oriented biosphere model. *Journal of Geophysical Research: Biogeosciences*, *120*(9), 1839–1857. https://doi.org/10.1002/2015JG002966

Baldocchi, D., Chu, H., & Reichstein, M. (2018). Inter-annual variability of net and gross ecosystem carbon fluxes: A review. *Agricultural and Forest Meteorology*, *249*, 520–533. https://doi.org/10.1016/j.agrformet.2017.05.015

Bauer, P., Thorpe, A., & Brunet, G. (2015). The quiet revolution of numerical weather prediction. *Nature*, *525*(7567), 45–55. https://doi.org/10.1038/nature14956

Beer, C., Reichstein, M., Tomelleri, E., Ciais, P., Jung, M., Carvalhais, N., Rödenbeck, C., Arain, M. A., Baldocchi, D., Bonan, G. B., Bondeau, A., Cescatti, A., Lasslop, G., Lindroth, A., Lomas, M., Luyssaert, S., Margolis, H., Oleson, K. W., Roupsard, O., … Papale, D. (2010). Terrestrial Gross Carbon Dioxide Uptake: Global Distribution and Covariation with Climate. *Science*, *329*(5993), 834–838. https://doi.org/10.1126/science.1184984

Bonan, Gordon. (2016). *Ecological Climatology: Concepts and Applications* (3rd ed.). Cambridge University Press.

Braswell, B. H., Sacks, W. J., Linder, E., & Schimel, D. S. (2005). Estimating diurnal to annual ecosystem parameters by synthesis of a carbon flux model with eddy covariance net ecosystem exchange observations. *Global Change Biology*, *11*(2), 335–355. https://doi.org/10.1111/j.1365-2486.2005.00897.x

Byrne, B., Liu, J., Bloom, A. A., Bowman, K. W., Butterfield, Z., Joiner, J., Keenan, T. F., Keppel-Aleks, G., Parazoo, N. C., & Yin, Y. (2020). Contrasting Regional Carbon Cycle Responses to Seasonal Climate Anomalies Across the East-West

Divide of Temperate North America. *Global Biogeochemical Cycles*, *34*(11), e2020GB006598. https://doi.org/10.1029/2020GB006598

Cowdery, E., Kooper, R., LeBauer, D., Desai, A. R., Mantooth, J., & Dietze, M. (2014). *The PEcAn Project: Accessible Tools for On-demand Ecosystem Modeling*. *2014*, B13C-0202.

Cranko Page, J., De Kauwe, M. G., Abramowitz, G., Cleverly, J., Hinko-Najera, N., Hovenden, M. J., Liu, Y., Pitman, A. J., & Ogle, K. (2022). Examining the role of environmental memory in the predictability of carbon and water fluxes across Australian ecosystems. *Biogeosciences*, *19*(7), 1913–1932. https://doi.org/10.5194/bg-19-1913-2022

Dietze. (2017a). *Ecological Forecasting*. Princeton University Press. https://press.princeton.edu/books/hardcover/9780691160573/ecological-forecasting

Dietze, M. C. (2017b). Prediction in ecology: A first-principles framework. *Ecological Applications*, *27*(7), 2048–2060. https://doi.org/10.1002/eap.1589

Dietze, M. C., Fox, A., Beck-Johnson, L. M., Betancourt, J. L., Hooten, M. B., Jarnevich, C. S., Keitt, T. H., Kenney, M. A., Laney, C. M., Larsen, L. G., Loescher, H. W., Lunch, C. K., Pijanowski, B. C., Randerson, J. T., Read, E. K., Tredennick, A. T., Vargas, R., Weathers, K. C., & White, E. P. (2018). Iterative near-term ecological forecasting: Needs, opportunities, and challenges. *Proceedings of the National Academy of Sciences of the United States of America*, *115*(7), 1424–1432.

Dokoohaki, H., Morrison, B. D., Raiho, A., Serbin, S. P., & Dietze, M. (2021). A novel model-data fusion approach to terrestrial carbon cycle reanalysis across the contiguous U.S using SIPNET and PEcAn state data assimilation system v. 1.7.2. *Geoscientific Model Development Discussions*, 1–28. https://doi.org/10.5194/gmd-2021-236

Fer, I., Gardella, A. K., Shiklomanov, A. N., Campbell, E. E., Cowdery, E. M., De Kauwe, M. G., Desai, A., Duveneck, M. J., Fisher, J. B., Haynes, K. D., Hoffman, F. M., Johnston, M. R., Kooper, R., LeBauer, D. S., Mantooth, J., Parton, W. J., Poulter, B., Quaife, T., Raiho, A., … Dietze, M. C. (2021). Beyond ecosystem modeling: A roadmap to community cyberinfrastructure for ecological data-model integration. *Global Change Biology*, *27*(1), 13–26. https://doi.org/10.1111/gcb.15409

Fer, I., Kelly, R., Moorcroft, P. R., Richardson, A. D., Cowdery, E. M., & Dietze, M. C. (2018). Linking big models to big data: Efficient ecosystem model calibration through Bayesian model emulation. *Biogeosciences*, *15*(19), 5801–5830. https://doi.org/10.5194/bg-15-5801-2018

Fer, I., Shiklomanov, A., Novick, K. A., Gough, C. M., Arain, M. A., Chen, J., Murphy, B., Desai, A. R., & Dietze, M. C. (2021). *Capturing site-to-site variability through Hierarchical Bayesian calibration of a process-based dynamic vegetation model* (p. 2021.04.28.441243). bioRxiv. https://doi.org/10.1101/2021.04.28.441243

Finzi, A. C., Giasson, M.-A., Barker Plotkin, A. A., Aber, J. D., Boose, E. R., Davidson, E. A., Dietze, M. C., Ellison, A. M., Frey, S. D., Goldman, E., Keenan, T. F., Melillo, J. M., Munger, J. W., Nadelhoffer, K. J., Ollinger, S. V., Orwig, D. A., Pederson, N., Richardson, A. D., Savage, K., … Foster, D. R. (2020). Carbon budget of the Harvard Forest Long-Term Ecological Research site: Pattern, process, and response to global change. *Ecological Monographs*, *90*(4), e01423. https://doi.org/10.1002/ecm.1423

Friedlingstein, P., Jones, M. W., O'Sullivan, M., Andrew, R. M., Bakker, D. C. E., Hauck, J., Le Quéré, C., Peters, G. P., Peters, W., Pongratz, J., Sitch, S., Canadell, J. G., Ciais, P., Jackson, R. B., Alin, S. R., Anthoni, P., Bates, N. R., Becker, M., Bellouin, N., … Zeng, J. (2022). Global Carbon Budget 2021. *Earth System Science Data*, *14*(4), 1917–2005. https://doi.org/10.5194/essd-14-1917-2022

Hicke, J. A., Asner, G. P., Randerson, J. T., Tucker, C., Los, S., Birdsey, R., Jenkins, J. C., Field, C., & Holland, E. (2002). Satellite-derived increases in net primary productivity across North America, 1982–1998. *Geophysical Research Letters*, *29*(10), 69-1-69–4. https://doi.org/10.1029/2001GL013578

Houghton, R. A. (2003). Revised estimates of the annual net flux of carbon to the atmosphere from changes in land use and land management 1850–2000. *Tellus B: Chemical and Physical Meteorology*, *55*(2), 378–390. https://doi.org/10.3402/tellusb.v55i2.16764

Hufkens, K., & Labs, B. (2023). *MODISTools: Interface to the "MODIS Land Products Subsets" Web Services* (1.1.4). https://cran.r-project.org/web/packages/MODISTools/index.html

Jordan, A., Krueger, F., & Lerch, S. (2020). *scoringRules: Scoring Rules for Parametric and Simulated Distribution Forecasts* (1.0.1). https://CRAN.R-project.org/package=scoringRules

LeBauer, D., Kooper, R., Mulrooney, P., Rohde, S., Wang, D., Long, S. P., & Dietze, M. C. (2018). BETYdb: A yield, trait, and ecosystem service database applied to second-generation bioenergy feedstock production. *GCB Bioenergy*, *10*(1), 61–71. https://doi.org/10.1111/gcbb.12420

LeBauer, D. S., Wang, D., Richter, K., Davidson, C., & Dietze, M. C. (2013). *Facilitating feedbacks between field measurements and ecosystem models* (1.7.2) [R]. https://doi.org/10.1890/12-0137.1 (Original work published 2012)

Leith, C. E. (1974). Theoretical Skill of Monte Carlo Forecasts. *Monthly Weather Review*, *102*(6), 409–418. https://doi.org/10.1175/1520-0493(1974)102<0409:TSOMCF>2.0.CO;2

Luo, Y., Keenan, T. F., & Smith, M. (2015). Predictability of the terrestrial carbon cycle. *Global Change Biology*, *21*(5), 1737–1751. https://doi.org/10.1111/gcb.12766

Lynch, P. (2008). The origins of computer weather prediction and climate modeling. *Journal of Computational Physics*, *227*(7), 3431–3444. https://doi.org/10.1016/j.jcp.2007.02.034

Moore, D. J. P., Hu, J., Sacks, W. J., Schimel, D. S., & Monson, R. K. (2008). Estimating transpiration and the sensitivity of carbon uptake to water availability in a subalpine forest using a simple ecosystem process model informed by measured net CO2 and H2O fluxes. *Agricultural and Forest Meteorology*, *148*(10), 1467–1477. https://doi.org/10.1016/j.agrformet.2008.04.013

Myneni, Ranga, Knyazikhin, Yuri, & Park, Taejin. (2015). *MOD15A2H MODIS/Terra Leaf Area Index/FPAR 8-Day L4 Global 500m SIN Grid V006* [Data set]. NASA EOSDIS Land Processes DAAC. https://doi.org/10.5067/MODIS/MOD15A2H.006

*NEON | Herbaceous clip harvest*. (n.d.). Retrieved May 9, 2022, from https://data.neonscience.org/data-products/DP1.10023.001

*NEON | Plant presence and percent cover*. (n.d.). Retrieved May 9, 2022, from https://data.neonscience.org/data-products/DP1.10058.001

*NEON | Soil physical and chemical properties, Megapit*. (n.d.). Retrieved May 9, 2022, from https://data.neonscience.org/data-products/DP1.00096.001

*NEON | Vegetation structure*. (n.d.). Retrieved May 9, 2022, from https://data.neonscience.org/data-products/DP1.10098.001

NOAA. (n.d.-a). *Climate Prediction Center—NMME Forecasts of Monthly Climate Anomalies* [Data set]. Retrieved June 23, 2023, from https://www.cpc.ncep.noaa.gov/products/NMME/

NOAA. (n.d.-b). *Climate Prediction Center—Outlooks: CFS Forecast of Seasonal Climate Anomalies* [Data set]. Retrieved June 23, 2023, from https://www.cpc.ncep.noaa.gov/products/CFSv2/CFSv2seasonal.shtml

NOAA. (n.d.-c). *Global Ensemble Forecast System (GEFS)*. NOAA, U.S. Department of Commerce.

Pastorello, G., Trotta, C., Canfora, E., Chu, H., Christianson, D., Cheah, Y.-W., Poindexter, C., Chen, J., Elbashandy, A., Humphrey, M., Isaac, P., Polidori, D., Reichstein, M., Ribeca, A., van Ingen, C., Vuichard, N., Zhang, L., Amiro, B., Ammann, C., … Papale, D. (2020). The FLUXNET2015 dataset and the ONEFlux processing pipeline for eddy covariance data. *Scientific Data*, *7*(1), Article 1. https://doi.org/10.1038/s41597-020-0534-3

Raiho, A., Dietze, M., Dawson, A., Rollinson, C. R., Tipton, J., & McLachlan, J. (2020). Towards understanding predictability in ecology: A forest gap model case study *bioRxiv* https://doi.org/10.1101/2020.05.05.079871

Sacks, W. J., Schimel, D. S., Monson, R. K., & Braswell, B. H. (2006). Model-data synthesis of diurnal and seasonal CO2 fluxes at Niwot Ridge, Colorado. *Global Change Biology*, *12*(2), 240–259. https://doi.org/10.1111/j.1365-2486.2005.01059.x

Smagorjnsky, J. (1983). The Beginnings of Numerical Weather Prediction and General Circulation Modeling: Early Recollections. In B. Saltzman (Ed.), *Advances in Geophysics* (Vol. 25, pp. 3–37). Elsevier. https://doi.org/10.1016/S0065-2687(08)60170-3

Stumpf, R. P., Tomlinson, M. C., Calkins, J. A., Kirkpatrick, B., Fisher, K., Nierenberg, K., Currier, R., & Wynne, T. T. (2009). Skill assessment for an operational algal bloom forecast system. *Journal of Marine Systems*, *76*(1), 151–161. https://doi.org/10.1016/j.jmarsys.2008.05.016

Thompson, P. D. (1957). Uncertainty of Initial State as a Factor in the Predictability of Large Scale Atmospheric Flow Patterns. *Tellus*, *9*(3), 275–295. https://doi.org/10.1111/j.2153-3490.1957.tb01885.x

Tian, Y., Xu, T., Chen, F., He, X., & Li, S. (2022). Can Data Assimilation Improve Short-Term Prediction of Land Surface Variables? *Remote Sensing*, *14*(20), Article 5172. https://doi.org/10.3390/rs14205172

White, E. P., Yenni, G. M., Taylor, S. D., Christensen, E. M., Bledsoe, E. K., Simonis, J. L., & Ernest, S. K. M. (2019). Developing an automated iterative near-term forecasting system for an ecological study. *Methods in Ecology and Evolution*, *10*(3), 332–344. https://doi.org/10.1111/2041-210X.13104

Wood, S. (2022). *mgcv: Mixed GAM Computation Vehicle with Automatic Smoothness Estimation* (1.8-40). https://CRAN.R-project.org/package=mgcv

Xing, X., Wu, M., Scholze, M., Kaminski, T., Vossbeck, M., Lu, Z., Wang, S., He, W., Ju, W., & Jiang, F. (2023). Soil Moisture Assimilation Improves Terrestrial Biosphere Model GPP Responses to Sub-Annual Drought at Continental Scale. *Remote Sensing*, *15*(3), Article 676. https://doi.org/10.3390/rs15030676

Zeng, N., Yoon, J.-H., Vintzileos, A., Collatz, G. J., Kalnay, E., Mariotti, A., Kumar, A., Busalacchi, A., & Lord, S. (2008). Dynamical prediction of terrestrial ecosystems and the global carbon cycle: A 25-year hindcast experiment. *Global Biogeochemical Cycles*, *22*(4). https://doi.org/10.1029/2008GB003183

Zhang, Hailing. Pu, Zhaoxia. (2010). Beating the Uncertainties: Ensemble Forecasting and Ensemble-Based Data Assimilation in Modern Numerical Weather Prediction. *Advances in Meteorology, 2010,* article 432160. https://www.hindawi.com/journals/amete/2010/432160/

Zobitz, J. M., Moore, D. J. P., Sacks, W. J., Monson, R. K., Bowling, D. R., & Schimel, D. S. (2008). Integration of process-based soil respiration models with whole-ecosystem CO2 measurements. *Ecosystems*, *11*(2), 250–269. https://doi.org/10.1007/s10021-007-9120-1

## CURRICULUM VITAE